ETH
Eidgenössische Technische Hochschule Zürich
Swiss Federal Institute of Technology Zurich

Seminar for Applied Mathematics SAM

Efficient computation of all speed flows using an entropy stable shock-capturing space-time discontinuous Galerkin method

A. Hiltebrand and S. Mishra

Research Report No. 2014-17
July 2014

Seminar für Angewandte Mathematik
Eidgenössische Technische Hochschule
CH-8092 Zürich
Switzerland

Funding ERC: 306279 SPARCCLE

EFFICIENT COMPUTATION OF ALL SPEED FLOWS USING AN ENTROPY STABLE SHOCK-CAPTURING SPACE-TIME DISCONTINUOUS GALERKIN METHOD.

A. HILTEBRAND AND S. MISHRA

Abstract. We present a shock-capturing space-time Discontinuous Galerkin method to approximate all speed flows modeled by systems of conservation laws with multiple time scales. The method provides a very general and computationally efficient framework for approximating such systems on account of its ability to incorporate large time steps. Numerical examples ranging from computing the incompressible limit (robustness with respect to Mach number) of the Euler equations to accelerating convergence to steady state are presented for illustrating the method.

1. Introduction

1.1. **The models.** Systems of conservation laws are *nonlinear* systems of partial differential equations that arise in a wide variety of problems in physics and engineering. Examples include the shallow water equations of oceanography, the Euler equations of compressible fluid dynamics, the MagnetoHydroDynamics (MHD) equations of plasma physics, and the equations of nonlinear elasticity [5].

A generic form for a multi-dimensional system of conservation laws is

$$\mathbf{U}_t + \sum_{k=1}^{d} \mathbf{F}^k(\mathbf{U})_{x_k} = 0, \quad (x,t) \in \Omega \times \mathbb{R}_+. \tag{1.1}$$

Here, $\Omega \subset \mathbb{R}^d$ $(d = 1, 2, 3)$ is a bounded spatial domain and $\mathbf{U} : \Omega \mapsto \mathbb{R}^m$ is the vector of unknowns. $\mathbf{F}^k$ is the (smooth) flux vector in the k-th direction. The conservation law (1.1) is equipped with suitable initial and boundary conditions.

The system (1.1) is termed *hyperbolic* if the flux Jacobian (along each normal direction) has real eigenvalues [5]. Hyperbolic systems are characterized by the fact that solutions of (1.1) can be expressed in terms of waves that travel at finite speeds. Furthermore, it is well known that solutions of (1.1) develop discontinuities such as *shock waves* in finite time, even when the initial data are smooth. Hence, the solutions of (1.1) are sought as integrable functions that satisfy (1.1) in the sense of distributions [5]. These *weak solutions* are not necessarily unique. Admissibility criteria in the form of *entropy conditions* need to be imposed in order to select a unique weak solution [5]. In fact, recent numerical work [14] indicates that an even weaker notion of solutions, that of *entropy measure valued solutions* [9], is an appropriate framework of solutions for (1.1).

1.2. **Numerical methods.** A large variety of numerical methods, such as finite volume, conservative finite difference, discontinuous Galerkin finite element and spectral viscosity methods, have been developed to efficiently approximate systems of conservation laws (1.1). Finite volume methods are often the preferred discretization framework [31]. Such methods rely on evolving the cell average of the solution of (1.1) in terms of numerical fluxes that are based on the exact (approximate) solutions of Riemann problems at each interface. Higher-order spatial accuracy is obtained by employing non-oscillatory piecewise polynomial reconstruction procedures such as TVD [31], ENO [20], and WENO [34]. An alternative high-order spatial discretization is provided by the Discontinuous Galerkin method [4].

Date: July 23, 2014.

1991 *Mathematics Subject Classification.* 65M60,35L65.

Acknowledgement. AH and SM were partially supported by ERC STG NN. 306279 SPARCCLE.

Although the above mentioned methods are highly successful and widely used, rigorous stability and convergence results, particularly for multi-dimensional systems of conservation laws, are lacking. Recently developed schemes as the TeCNO schemes [13] combine arbitrary high-order of accuracy with entropy stability (the only known notion of nonlinear stability for systems of conservation laws). Furthermore, these schemes can be shown to converge to entropy measure valued solutions of (1.1) [14].

1.2.1. *Time stepping.* Hyperbolic conservation laws are characterized by finite speeds of propagation. Hence and in contrast with parabolic problems, explicit time stepping methods are often employed for time integration of the high-resolution finite volume and DG schemes. A particularly attractive choice are the strong stability preserving (SSP) Runge-Kutta methods [16]. Alternatives include the ADER time stepping procedure [37]. The time step in explicit methods is related to the spatial mesh size in terms of *fastest wave speed* of the hyperbolic system (1.1) [31].

1.3. **Multiple time scales.** The $m \times m$ hyperbolic system (1.1) possesses m different waves traveling at different speeds. In many problems of interest, these wave speeds can differ by several orders of magnitude, resulting in the presence of multiple time scales in the system. A prototypical example for such systems is the *incompressible limit of the Euler equations* [31]. It is well known that solutions to the Euler equations contain acoustic waves and matter waves (density fluctuations, contact discontinuities, and velocity shear waves). The Mach number characterizes the difference in amplitude between these two families of waves. The incompressible limit is determined letting the Mach number go to zero. In this regime, the small density fluctuations ensure that the acoustic waves are orders of magnitude faster than the matter waves. However, it is only the matter waves that carry significant information about the incompressible limit.

The numerical resolution of the incompressible limit by standard explicit (such as the SSP-RK) time stepping methods is notoriously difficult ([31] and references therein) as the time step in such methods is dictated by the very fast moving acoustic waves. The resulting time step can be very small and the overall computational cost prohibitively expensive, particularly as the resolution of these time scales (corresponding to the fast acoustic waves) is of little interest.

Another prototypical example for a system with multiple time scales is given by Radiation hydrodynamics and Radiation MHD ([15]). Again, the fastest time scale in the system is dictated by the radiation waves that travel at the speed of light. However, these waves carry little information and the main objective of any simulation is to approximate the time scales corresponding to the sonic and magneto-sonic waves, that are $4-5$ orders of magnitude slower than the light waves. Multiphase flows also contain such examples of systems with multiple time scales, [10] and references therein.

As a final example of systems with multiple time scales, we can also include systems of conservation laws where the steady state is the main interest of the computation, for instance in aerodynamic calculations [21]. One of the standard approaches for computing steady states is to start the computation with some initial conditions and drive the system to converge to steady state. The time evolution to steady state, if computed by an explicit method, is again enormously expensive as the time step can be very small. Furthermore, the computation of the transient is of little significance as we are interested in only the steady state.

The above examples illustrate that when a system of conservation laws contains multiple time scales that differ in orders of magnitude, one is mainly interested in resolving the slow time scales. Explicit methods, that are designed to resolve the fastest time scale, are very expensive computationally when they are employed to approximate such *all speed flows* and an alternative framework needs to be designed.

1.4. **A brief survey of existing methods to compute all speed flows.** A large number of methods have been developed to deal with multiple time scales in conservation laws. An overarching feature of these methods is that almost all of them are designed with a specific application in mind. In particular, efficient computation of the incompressible limit of the compressible Euler equations has received a lot of attention beginning with the implicit continuous fluid Eulerian (ICE) technique of Harlow and Amsdan [18, 19]. These methods use incompressible techniques such as staggered meshes to simulate compressible flows in the low mach number limit. Other popular methods include the splitting methods of Bijl and Wesseling [3], the multiple pressure variable methods of Munz et al [32, 33], the asymptotic preserving (AP) methods of Degond, Jin, Liu, and

co-workers [8, 6, 7, 17] and references therein, semi-implicit methods of Klein and co-workers [29, 30] and the conservative pressure methods of Huel and Wesseling [38].

Similarly, a large number of semi-implicit numerical methods have been developed to deal with Radiation hydrodynamics and Radiation Magnetohydrodynamics (see [15] for a literature survey of these methods). A literature survey for methods to compute all speed multiphase flows is given in [10]. Finally, accelerating convergence to steady state in aerodynamic simulations has been considered in the pioneering works of Jameson [26].

The wide variety of methods described above employ some form of implicit and semi-implicit time stepping in order to factor out the fast waves of the system and resolve the slow waves of interest. The methodologies are mostly of an adhoc nature and work well for particular applications. It would be fair to say that there is scope to develop a broad-based and fairly general numerical method that is able to approximate the system of conservation laws (1.1) in a stable and efficient manner while being robust to the presence of multiple time scales in the system. We aim to describe such a numerical method in this paper.

1.5. **Aims and scope of the current paper.** The main aim of the current paper is to present a robust numerical method for approximating (1.1) that can efficiently compute all speed flows ranging from the incompressible limit of the Euler equations to convergence to steady state in aerodynamical calculations. Our method is a space-time Discontinuous Galerkin (DG) method that was described in a recent paper [22]. In turn, this method was based on earlier works such as [28, 27, 2]. The method is based on the discretization of the space-time computational domain into finite elements and the subsequent approximation of a suitable variational formulation of the system of conservation laws (1.1). Entropy variables are the degrees of freedom of the variational formulation. Suitable numerical fluxes (those designed by Tadmor in [36], see also [13]) are employed to ensure nonlinear entropy stability. Further stabilization operators such as streamline diffusion as well as shock-capturing operators ensure sufficient intra-element stabilization and (essentially) oscillation free shock-capturing. The method was presented in [22] and was shown to be entropy stable as well as convergent to an entropy measure valued solution of the conservation law (1.1). The design of efficient preconditioners for the method was the subject of another recent paper [23] and space-time adaptivity aspects of the method are presented in [24].

As shown in [22], the space-time DG method is unconditionally stable i.e., entropy stability holds without any restriction on the time step. In particular, the time step is not bound by the fastest wave speed of the system (1.1). Given this observation, the shock-capturing space-time DG method can be readily adapted for the computation of all speed flows (multiple time scales) by setting the time step such that only the time scales corresponding to the slow waves of interest need to be resolved. Hence, the fastest waves that impede computational efficiency can be factored out automatically in this method. We present this approach in the current paper and illustrate its success with a large number of numerical experiments

The rest of the paper is organized as follows: in section 2, we present the shock-capturing space-time DG method. The general methodology for computing all speed flows is presented in section 3 and is illustrated for a model linear hyperbolic system in section 4. In section 5, we present numerical examples for all speed flows modeled by the Euler equations of gas dynamics.

2. The shock-capturing space-time DG method

Following the recent paper [22], we assume that the system of conservation laws (1.1) is equipped with a convex entropy function $S : \mathbb{R}^m \mapsto \mathbb{R}$ and the corresponding entropy variables are $\mathbf{V} = S_{\mathbf{U}}$. As S is convex, the mapping $\mathbf{V} = \mathbf{V}(\mathbf{U})$ is invertible [5] and the conservation law (1.1) can be expressed in terms of the vector of entropy variables $\mathbf{V}$ as,

$$\mathbf{U}(\mathbf{V})_t + \sum_{k=1}^{d} \mathbf{F}^k(\mathbf{V})_{x_k} = 0, \quad (x,t) \in \Omega \times \mathbb{R}_+, \tag{2.1}$$

Here, we have used the change of variable $\mathbf{U} = \mathbf{U}(\mathbf{V})$ and retained the notation $\mathbf{F}^k(\mathbf{V}) = \mathbf{F}^k(\mathbf{U}(\mathbf{V}))$ for all k, for notational convenience. This is the form of the conservation law that we are going to discretize using a space-time DG method.

2.1. **The mesh.** At the n-th time level t^n, we denote the time step as $\Delta t^n = t^{n+1} - t^n$ and the update time interval as $I^n = [t^n, t^{n+1})$. For simplicity, we assume that the spatial domain $\Omega \subset \mathbb{R}^d$ is polyhedral and divide it into a triangulation $\mathcal{T}$, i.e., a set of open convex polyhedra $K \subset \mathbb{R}^d$ with plane faces. Furthermore, we assume mesh regularity [27] and quasiuniformity. For a generic element (cell) K, we denote

$$\begin{aligned}\Delta x_K &= \operatorname{diam}(K),\\ \mathcal{N}(K) &= \{K' \in \mathcal{T} : K' \neq K \wedge \operatorname{meas}_{d-1}(\overline{K} \cap \overline{K'}) > 0\}.\end{aligned}$$

The *mesh width* of the triangulation is $\Delta x(\mathcal{T}) = \max_K \Delta x_K$. A generic spacetime element is the prism:

$$K \times I^n.$$

We also assume that there exists an (arbitrarily large) constant $C > 0$ such that

$$(1/C)\Delta x \leq \Delta t^n \leq C \Delta x, \tag{2.2}$$

for all time levels n.

2.2. **Variational formulation.** On a given triangulation $\mathcal{T}$ with mesh width Δx, we seek entropy variables

$$\begin{aligned}\mathbf{V}^{\Delta x} \in \mathcal{V}_p &= (\mathbb{P}_p(\Omega \times [0,T]))^m\\ &= \{\mathbf{W} \in \left(L^1(\Omega \times [0,T])\right)^m : \mathbf{W}|_{K \times I^n} \quad \text{is a polynomial of degree } p \text{ in each component}\}\end{aligned} \tag{2.3}$$

such that the following quasilinear variational form is satisfied for each $\mathbf{W}^{\Delta x} \in \mathcal{V}_p$:

$$\mathcal{B}(\mathbf{V}^{\Delta x}, \mathbf{W}^{\Delta x}) := \mathcal{B}_{DG}(\mathbf{V}^{\Delta x}, \mathbf{W}^{\Delta x}) + \mathcal{B}_{SD}(\mathbf{V}^{\Delta x}, \mathbf{W}^{\Delta x}) + \mathcal{B}_{SC}(\mathbf{V}^{\Delta x}, \mathbf{W}^{\Delta x}) = 0. \tag{2.4}$$

We elaborate on each of the three quasilinear forms (nonlinear in the first argument and linear in the second) in the following.

2.3. **The DG quasilinear form.** The form $\mathcal{B}_{DG}$ is given by,

$$\begin{aligned}\mathcal{B}_{DG}(\mathbf{V}^{\Delta x}, \mathbf{W}^{\Delta x}) = &-\sum_{n,K} \int_{I^n} \int_K \left(\left\langle \mathbf{U}(\mathbf{V}^{\Delta x}), \mathbf{W}_t^{\Delta x} \right\rangle + \sum_{k=1}^d \left\langle \mathbf{F}^k(\mathbf{V}^{\Delta x}), \mathbf{W}_{x_k}^{\Delta x} \right\rangle \right) dx dt\\ &+ \sum_{n,K} \int_K \left\langle \mathbb{U}(\mathbf{V}_{n+1,-}^{\Delta x}, \mathbf{V}_{n+1,+}^{\Delta x}), \mathbf{W}_{n+1,-}^{\Delta x} \right\rangle dx - \sum_{n,K} \int_K \left\langle \mathbb{U}(\mathbf{V}_{n,-}^{\Delta x}, \mathbf{V}_{n,+}^{\Delta x}), \mathbf{W}_{n,+}^{\Delta x} \right\rangle dx\\ &+ \sum_{n,K} \sum_{K' \in \mathcal{N}(K)} \int_{I^n} \int_{\partial_{KK'}} \left(\sum_{k=1}^d \left\langle \mathbb{F}^{k,*}(\mathbf{V}_{K,-}^{\Delta x}, \mathbf{V}_{K,+}^{\Delta x}), \mathbf{W}_{K,-}^{\Delta x} \right\rangle \nu_{KK'}^k \right) d\sigma(x) dt\\ &- \frac{1}{2} \sum_{n,K} \sum_{K' \in \mathcal{N}(K)} \int_{I^n} \int_{\partial_{KK'}} \left\langle \mathbf{W}_{K,-}^{\Delta x}, \mathbf{D}(\mathbf{V}_{K,+}^{\Delta x} - \mathbf{V}_{K,-}^{\Delta x}) \right\rangle d\sigma(x) dt.\end{aligned} \tag{2.5}$$

Here we have employed the notation,

$$\begin{aligned}\mathbf{W}_{n,\pm}(x) &= \mathbf{W}(x, t_\pm^n),\\ \partial_{KK'} &= \overline{K} \cap \overline{K'},\\ \nu_{KK'} &= \text{unit normal for edge KK}' \text{ pointing outwards from element K},\\ \mathbf{W}_{K,\pm}(x,t) &= \lim_{h \to 0} \mathbf{W}(x \pm h\nu, t), \quad \forall x \in \partial_{KK'},\\ \mathbf{D} &= \mathbf{D}(\mathbf{V}_{K,-}^{\Delta x}, \mathbf{V}_{K,+}^{\Delta x}; \nu_{KK'})\end{aligned}$$

for all $\mathbf{W} \in \mathcal{V}_p$. We remark that the boundary condition is ignored in the above variational form by considering compactly supported (in the spatial domain) solutions and test functions.

2.3.1. *Numerical fluxes.* Both the temporal and spatial numerical fluxes, need to be specified in order to complete the DG quasilinear form. In order to obtain causality (marching) after each time step, we choose the temporal numerical flux to be the *upwind* flux:

$$\mathbb{U}(a,b) = \mathbf{U}(a). \tag{2.6}$$

This ensures that we can use the values at the previous time step in order to compute an update at the time level t^n. A different choice of temporal numerical fluxes will imply that all the degrees of freedom (for all times) are coupled and force us to solve a very large non-linear algebraic system of equations.

The spatial numerical flux consists of the following two components,

2.3.2. *Entropy conservative flux:* The entropy conservative flux (in the k-th direction) is any flux [35] that satisfies the relation:

$$\langle b-a, \mathbb{F}^{k,*}(a,b)\rangle = \Psi^k(b) - \Psi^k(a). \tag{2.7}$$

Here, $\Psi^k = \langle \mathbf{V}, \mathbf{F}^k\rangle - Q^k$ is the entropy potential. The existence of such fluxes (for any generic conservation law with an entropy framework) was shown by Tadmor in [35]. More recently, explicit expressions of entropy conservative fluxes for specific systems of interest like the shallow water equations [12] and Euler equations [25] have been obtained.

2.3.3. *Numerical diffusion operators:* Following [36, 12, 13], we choose the numerical diffusion operator as,

$$\mathbf{D}(a,b;\nu) = \mathbf{R}_\nu \mathbf{P}(\Lambda_\nu(\cdot);a,b)\mathbf{R}_\nu^\top. \tag{2.8}$$

Here, $\Lambda_\nu, \mathbf{R}_\nu$ are the eigenvalue and eigenvector matrices of the Jacobian $\partial_{\mathbf{U}}(\langle \mathbf{F}, \nu\rangle)$ in the normal direction ν. $\mathbf{R}_\nu$ is evaluated at an averaged state, e.g. $(a+b)/2$, and scaled such that $\mathbf{R}_\nu \mathbf{R}_\nu^\top = \mathbf{U}_{\mathbf{V}}$. $\mathbf{P}$ is a non-negative matrix function. Examples of $\mathbf{P}$ include $\mathbf{P}(\Lambda_\nu(\cdot);a,b) = |\Lambda_\nu(\frac{a+b}{2})|$, which leads to a Roe type scheme, and $\mathbf{P}(\Lambda_\nu(\cdot);a,b) = \max\{\lambda_{\max}(a;\nu), \lambda_{\max}(b;\nu)\}\mathbf{ID}$, which leads to a Rusanov type scheme [13], where $\lambda_{\max}(\mathbf{U};\nu)$ is the maximal wave speed in direction of ν, i.e. $\lambda_{\max}(\mathbf{U};\nu)$ is the spectral radius of $\Lambda_\nu(\mathbf{U})$.

2.4. **Streamline diffusion operator.** There is no numerical diffusion in the interior of the space-time element $K \times I^n$. In order to suppress the resulting unphysical oscillations near shocks, we choose the following streamline diffusion operator,

$$\mathcal{B}_{SD}(\mathbf{V}^{\Delta x}, \mathbf{W}^{\Delta x}) = \sum_{n,K} \int_{I^n}\int_K \left\langle \left(\mathbf{U}_{\mathbf{V}}(\mathbf{V}^{\Delta x})\mathbf{W}_t^{\Delta x} + \sum_{k=1}^d \mathbf{F}_{\mathbf{V}}^k(\mathbf{V}^{\Delta x})\mathbf{W}_{x_k}^{\Delta x}\right), \mathbf{D}^{SD}\mathrm{Res}\right\rangle dxdt \tag{2.9}$$

with intra-element residual:

$$\mathrm{Res} = \mathbf{U}(\mathbf{V}^{\Delta x})_t + \sum_{k=1}^d \mathbf{F}^k(\mathbf{V}^{\Delta x})_{x_k}, \tag{2.10}$$

and the scaling matrix is chosen as

$$\mathbf{D}^{SD} = C^{SD}\Delta t^n \mathbf{U}_{\mathbf{V}}^{-1}(\mathbf{V}^{\Delta x}), \tag{2.11}$$

for some positive constant C^{SD}. Note that the intra-element residual is well defined as we are taking first-derivatives of a polynomial function.

2.5. **Shock capturing operator.** The streamline diffusion operator adds numerical diffusion in the direction of the streamlines. However, we need further numerical diffusion in order to reduce possible oscillations at shocks. We use the following shock-capturing operator:

(2.12a)

$$\mathcal{B}_{SC}(\mathbf{V}^{\Delta x}, \mathbf{W}^{\Delta x}) = \sum_{n,K} \int_{I^n}\int_K D_{n,K}^{SC}\left(\left\langle \mathbf{W}_t^{\Delta x}, \mathbf{U}_{\mathbf{V}}(\tilde{\mathbf{V}}_{n,K})\mathbf{V}_t^{\Delta x}\right\rangle + \sum_{k=1}^d \frac{{\Delta x_K}^2}{(\Delta t^n)^2}\left\langle \mathbf{W}_{x_k}^{\Delta x}, \mathbf{U}_{\mathbf{V}}(\tilde{\mathbf{V}}_{n,K})\mathbf{V}_{x_k}^{\Delta x}\right\rangle\right) dxdt,$$

with

$$\tilde{\mathbf{V}}_{n,K} = \frac{1}{\mathrm{meas}(I^n \times K)}\int_{I^n}\int_K \mathbf{V}^{\Delta x}(x,t)dxdt.$$

being the cell average and the scaling factor,

$$D^{SC}_{n,K} = \frac{\Delta t^n C^{SC} \overline{\mathrm{Res}}_{n,K}}{\sqrt{\int_{I^n}\int_K \left(\left\langle \mathbf{V}_t^{\Delta x}, \mathbf{U}_{\mathbf{V}}(\tilde{\mathbf{V}}_{n,K})\mathbf{V}_t^{\Delta x} \right\rangle + \sum_{k=1}^{d} \frac{{\Delta x_K}^2}{(\Delta t^n)^2} \left\langle \mathbf{V}_{x_k}^{\Delta x}, \mathbf{U}_{\mathbf{V}}(\tilde{\mathbf{V}}_{n,K})\mathbf{V}_{x_k}^{\Delta x} \right\rangle \right) dxdt + \epsilon}}, \tag{2.12b}$$

with $\epsilon = |K|^{\frac{1}{2}} (\Delta t^n)^{\frac{-1}{2}} \left(\frac{\Delta x}{\mathrm{diam}(\Omega)} \right)^{\theta}$ and $\theta \geq 1/2$ (chosen as 1) and

$$\overline{\mathrm{Res}}_{n,K} = \sqrt{\int_{I^n}\int_K \left\langle \mathrm{Res}, \mathbf{U}_{\mathbf{V}}^{-1}(\mathbf{V}^{\Delta x})\mathrm{Res} \right\rangle dxdt}. \tag{2.12c}$$

Here, C^{SC} is a positive constant.

2.6. **Entropy stability and convergence.** The entire design of the shock-capturing space-time DG method (2.4) is motivated by the need to prove entropy stability for nonlinear conservation laws. To this end, we proved the following theorem in the recent paper [22]:

Theorem 2.1. *Consider the system of conservation laws* (1.1) *with strictly convex entropy function S and entropy flux functions Q^k $(1 \leq k \leq d)$. For simplicity, assume that the exact and approximate solutions have compact support inside the spatial domain Ω. Let the final time be denoted by t^N. Then, the streamline diffusion shock-capturing Discontinuous Galerkin scheme* (2.4) *approximating* (1.1) *has the following properties:*

(i.) The scheme (2.4) *is conservative i.e., the approximate solutions $\mathbf{U}^{\Delta x} = \mathbf{U}(\mathbf{V}^{\Delta x})$ satisfy*

$$\int_\Omega \mathbf{U}^{\Delta x}(x, t^N_-)dx = \int_\Omega \mathbf{U}^{\Delta x}(x, t^0_-)dx. \tag{2.13}$$

(ii.) The scheme (2.4) *is entropy stable i.e., the approximate solutions satisfy,*

$$\int_\Omega S(\mathbf{U}^*(t^0_-))dx \leq \int_\Omega S(\mathbf{U}^{\Delta x}(x, t^N_-))dx \leq \int_\Omega S(\mathbf{U}^{\Delta x}(x, t^0_-))dx, \tag{2.14}$$

with $\mathbf{U}^*$ being the domain average:

$$\mathbf{U}^*(t^0_-) = \frac{1}{\mathrm{meas}(\Omega)} \int_\Omega \mathbf{U}(\mathbf{V}(x, t^0_-))dx.$$

Hence, the space-time DG method is nonlinearly stable for any system of conservation laws that is equipped with a convex entropy function. The convexity of the entropy readily implies that the approximate solution $\mathbf{U}^{\Delta x}$ is bounded in L^2. Furthermore, under the additional assumption that the approximate solutions are bounded (uniformly) in L^∞, we proved that the approximate solutions converge to an entropy measure valued solution of the system of conservation laws (1.1) when $\Delta x \to 0$. Entropy measure valued solutions are a weaker but possibly more relevant solution concept for systems of conservation laws than entropy solutions [14]. Moreover, one can show that the approximate solutions converge to the weak solution of a linear symmetrizable system as well as to a weak solution for scalar conservation laws, see [24].

3. Methodology for computing all speed flows

We remark that the entropy stability result (Theorem 2.1) as well as the convergence results *do not* require any restriction on the time step Δt, apart from the very mild mesh regularity requirement (2.2). Note that the constant C in (2.2) can have any finite value. Thus, the method (2.4) is unconditionally stable with respect to time step size. Nevertheless, it is customary to relate the time step and the (spatial) mesh size (for the purpose of accuracy of the approximation) through a CFL type condition (see [22]),

$$\Delta t^n \leq C^{\mathrm{CFL}} \min_{K \in \mathcal{T}, x \in K} \frac{\Delta x_K}{\lambda_{\max}(\mathbf{U}^{\Delta x}(x, t^n))}, \tag{3.1}$$

in one space dimension and

$$\Delta t^n \leq C^{\mathrm{CFL}} \min_{K\in\mathcal{T}, x\in K} \frac{\frac{|K|}{\Delta x_K}}{\lambda_{\max}(\mathbf{U}^{\Delta x}(x,t^n))}, \tag{3.2}$$

in two space dimensions. Here $\lambda_{\max}(\mathbf{U}) = \max_\nu \lambda_{\max}(\mathbf{U};\nu)$ is the maximal wave speed (eigenvalue of the flux Jacobian) in all directions.

Note that the CFL number C^{CFL} can be taken arbitrarily large and the stability result still holds. However, accuracy may suffer from a large CFL number as the temporal error is $\mathcal{O}(\Delta t^s)$, with s being related to the order of the method (degree of the underlying polynomials) and a large C^{CFL} results in a large time step Δt and consequently, a possibly large error.

However and as mentioned in the introduction, there is a large class of problems with multiple time scales where the waves of interest travel with a speed bounded by $\lambda_{\max}^{\mathrm{slow}}$ and

$$\lambda_{\max}^{\mathrm{slow}} << \lambda_{\max}. \tag{3.3}$$

In other words, the fastest wave speed is considerably larger than the slow wave speed in the system. On the other hand, the interest of the computation is to compute the slow waves. For instance, the matter (shear) waves are much more relevant than the acoustic waves in the incompressible limit of the Euler equations [7]. Given this context, we take advantage of (3.3) and change the time step sizes (3.1) and (3.2) and set,

$$\Delta t^n \leq C_{red}^{\mathrm{CFL}} \min_{K\in\mathcal{T}, x\in K} \frac{\Delta x_K}{\lambda_{\max}^{\mathrm{slow}}(\mathbf{U}^{\Delta x}(x,t^n))}, \tag{3.4}$$

in one space dimension and

$$\Delta t^n \leq C_{red}^{\mathrm{CFL}} \min_{K\in\mathcal{T}, x\in K} \frac{\frac{|K|}{\Delta x_K}}{\lambda_{\max}^{\mathrm{slow}}(\mathbf{U}^{\Delta x}(x,t^n))}, \tag{3.5}$$

in two space dimensions.

From (3.1) (resp. (3.2)) and (3.4) (resp. (3.5)), we obtain that

$$C^{\mathrm{CFL}} \approx C_{red}^{\mathrm{CFL}} \frac{\lambda_{\max}}{\lambda_{\max}^{\mathrm{slow}}}. \tag{3.6}$$

We typically choose $C_{red}^{\mathrm{CFL}} = \mathcal{O}(1)$ (for the sake of high accuracy). Hence, from (3.6), we see that the effective CFL number C^{CFL} can be very large on account of (3.3). The resulting method has the following features,

- Unconditional stability of the space-time DG method implies that the effective CFL number C^{CFL} can be arbitrarily high and the method will still be stable.
- The fact that our interest is in resolving the slow waves of the system implies that the numerical error due to time discretization will still be low as the time step is based on the slow wave speed.
- The computational cost will be low as the slow wave speed is considerably smaller than the fast wave speed. This results in large time steps and significantly reduces the number of time steps that are required to reach the desired final time.

Hence, the shock-capturing DG method (2.4) with the time step decided by (3.4), (3.5) is well poised to resolve all speed flows efficiently. The method is readily modified to approximate convergence to steady state also.

3.1. **Brief description of implementation.** The implementation of the shock-capturing space-time DG method is described in detail in the recent paper [23], see also [24]. As the test and trial spaces for (2.4) involve piecewise polynomials, we choose a suitable basis for this space as the span of scaled and shifted monomials, see [23]. Then, the space-time DG formulation is recast into a large system of nonlinear algebraic equations for the degrees of freedom (entropy variables). Given the upwind temporal flux (2.6), one can perform time marching i.e., the degrees of freedom for a given time slab can be solved once the degrees of freedom for the previous time slab have been computed. Nevertheless, a large nonlinear algebraic system needs to be solved at every time step. We employ a damped Newton method to solve this nonlinear system (see [23]).

Given the structure of the Newton method, a large, sparse and non-symmetric linear system needs to be inverted at every step of the Newton iterate. This linear system is solved using an iterative procedure such as

GMRES. Such iterative schemes rely on the availability of efficient preconditioners to ensure convergence within a reasonable number of iterations. We have designed and analyzed efficient block Jacobi and block Gauss-Seidel preconditioners for this purpose. These preconditioners are also described in [23].

4. A toy model: Linear symmetric system involving two wave speeds

Next, we will investigate whether our general methodology, as presented in the last section, is able to efficiently approximate all speed flows modeled by systems of conservation laws such as (1.1). To this end, we consider a simple one-dimensional linear symmetric 2×2 system of the form:

$$\mathbf{U}_t + \mathbf{F}(\mathbf{U})_x = 0, \tag{4.1}$$

with

$$\mathbf{U} = \begin{pmatrix} u_1 \\ u_2 \end{pmatrix}, \quad \mathbf{F}(\mathbf{U}) = \frac{1}{2} \begin{pmatrix} (a+b)u_1 + (b-a)u_2 \\ (b-a)u_1 + (a+b)u_2 \end{pmatrix}. \tag{4.2}$$

Here, a and b are assumed to be positive constants with $a \leq b$. Clearly, the above system (4.1) is hyperbolic and has two wave speeds given by a and b. Based on our assumptions, $a \leq b$, we denote $\lambda_{\max} = b$ and $\lambda_{\max}^{\text{slow}} = a$. Furthermore, the energy $\frac{1}{2}\langle \mathbf{U}, \mathbf{U} \rangle$ serves as the canonical entropy for linear symmetric systems. Hence, the entropy variables $\mathbf{V} = \mathbf{U}$, coincide with the conservative variables.

We will apply the shock-capturing space-time DG method (2.4) to approximate the linear system (4.1). The only parameter that needs to be specified is the spatial numerical flux. It is well known (see [13]) that the entropy conservative flux (2.7) for linear systems is the arithmetic average of the two interfacial states. We will consider both the Rusanov diffusion operator with the wave speed being $\lambda = a$ as well as the Roe type diffusion operator in the numerical diffusion operator (2.8). Note that the Roe type diffusion operator, together with the arithmetic average as the entropy conservative flux, implies that the spatial numerical flux is the upwind flux for this linear system.

We consider (4.1) in the domain $[-1, 1]$ with initial Riemann data,

$$\begin{aligned} u_1(x,0) &= \begin{cases} 1, & x < 0 \\ 0, & x \geq 0 \end{cases} \\ u_2(x,0) &= 0. \end{aligned} \tag{4.3}$$

In the first numerical experiment, we would like to investigate whether the shock-capturing space-time DG method (2.4) can approximate a flow with vastly different wave speeds (time scales). To this end, we set $a = 1$ and $b = 100$ in (4.1). Thus, there is a slow wave traveling at speed 1 and a fast wave traveling at speed 100. Our interest is in computing the slow moving wave accurately as the fast wave quickly exits the domain. We set Dirichlet boundary conditions on the left boundary and Neumann type transparent boundary conditions on the right boundary. The exact solution can be readily computed by a characteristic decomposition of the system (4.1). We plot this exact solution at time $T = 0.5$ in figure 1. As seen in the figure, the fast wave, traveling at a speed 100, has clearly exited the computational domain and the slow wave has moved the initial discontinuity to 0.5.

To simulate this example, we use the shock-capturing space-time DG method (2.4) with the time step being determined by the condition (3.4) with $\lambda_{\max}^{\text{slow}} = a$. We set $C_{red}^{\text{CFL}} = 0.5$ and from (3.6), we see that the effective CFL number is $C^{\text{CFL}} = 50$. The results obtained with a piecewise quadratic ($p = 2$) elements and a Roe type numerical diffusion operator in (2.4), at different mesh resolutions, are plotted in figure 1. The figure clearly shows that the space-time DG method (1.1), even at a high CFL number of 50, is able to resolve both components of the solution very sharply. As expected, there are very small and localized oscillations near the discontinuities but the overall quality of approximation is really good, even for such large time steps as dictated by an effective CFL number of 50.

4.0.1. *Approximation of fast waves.* The aim of the above computation was to approximate the slow waves accurately as the fast waves have already exited the system. In order to explore the approximation of fast waves, we enlarge the computational domain to $(-1, 10)$ and compute only to the final time $T = 0.05$. In this case, the fast wave does not leave the domain. The results with same parameters as the previous example

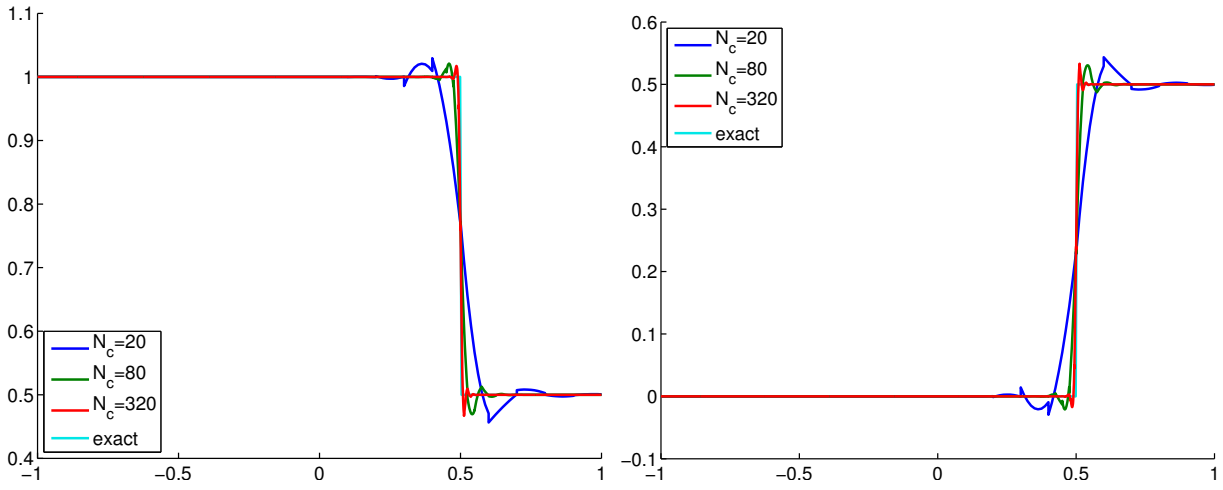

(a) u_1 (b) u_2

FIGURE 1. Approximate solution of (4.1) at time $T = 0.5$ with Neumann boundary conditions, for the two speed advection problem using polynomial degree $p = 2$, Roe type numerical diffusion operator and a fast wave speed of $b = 100$.

are shown in figure 2. We clearly see that the slow wave is sharply resolved, even at coarse mesh resolutions. However, the fast wave is diffused (smeared) by the approximation. This is not unexpected as the whole design of the method was to resolve slow waves accurately at the expense of smearing (inaccurate resolution) of fast waves.

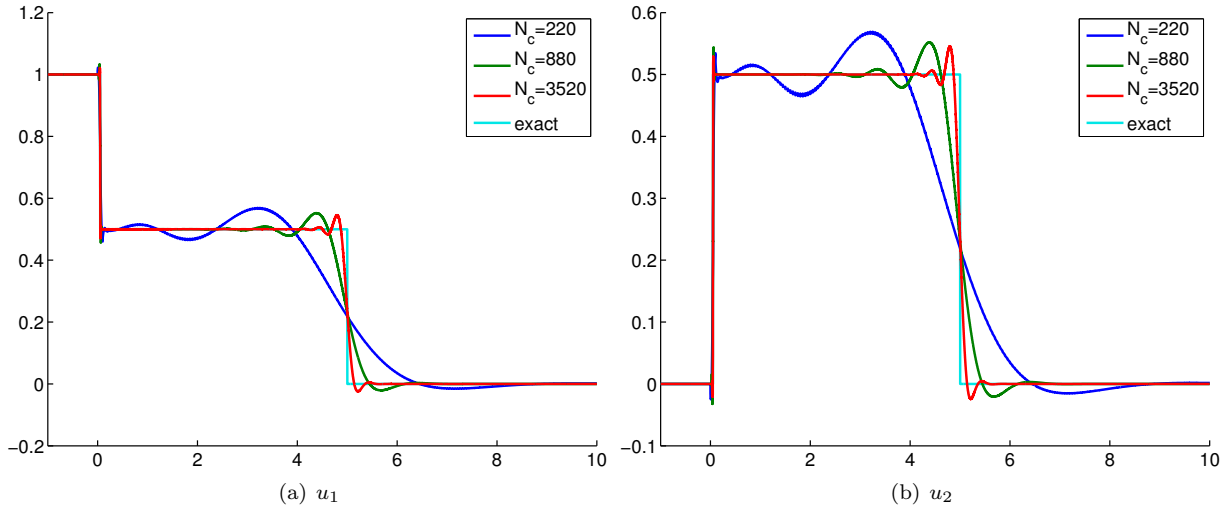

(a) u_1 (b) u_2

FIGURE 2. Approximate solution of (4.1) at time $T = 0.05$ on a larger domain using $p = 2$, Roe type numerical diffusion operator, and $b = 100$.

4.0.2. *Computational efficiency.* The results, shown in figure 1 clearly establish that the method is able to approximate the waves of interest (slow waves) accurately even at a high effective CFL number of 50. It is natural to examine if this high accuracy, even for large time steps, comes at a computational cost. Given

the nature of the shock-capturing space-time DG method (2.4), we need to solve a large nonlinear system of equations at every time step even though the underlying PDE (4.1) is linear. The Newton method converged to the desired tolerance within three iterations for this problem. Thus, the main contributor to the computational cost per time step, was the GMRES solve per Newton iterate. As described in detail in [23] and mentioned in the last section, we will employ block Jacobi and block Gauss-Seidel preconditioners for GMRES. The average number of iterations for the preconditioned GMRES to converge is presented in figure 3. We compare three different cases, that of $b = 1$, 10, and 100, i.e., when there is no separation, intermediate separation, and a large separation in wave speeds (time scales) for the system (4.1). The results obtained with a Roe type numerical diffusion operator are presented in figure 3 and show that

- The number of iterations (wrt both preconditioners) is approximately independent of the mesh resolution.
- There is very little difference between the number of iterations between piecewise linear ($p = 1$) and piecewise quadratic ($p = 2$) elements.
- The block Gauss-Seidel preconditioner converges in one iteration, irrespective of mesh size, polynomial degree, or effective CFL number (size of the time step). This is on account of the fact that the Gauss-Seidel preconditioner amounts to a direct solve for an upwind flux [23].
- There is a very modest (at most three fold) increase in the number of iterations for the block Jacobi preconditioner even when the size of time step (effective CFL number) changes by two orders of magnitude.

Given the above observations, we conclude that there is very little increase in computational cost per time step, even when the time step size increases by two orders of magnitude. Thus, for large time step sizes, the method is computationally efficient.

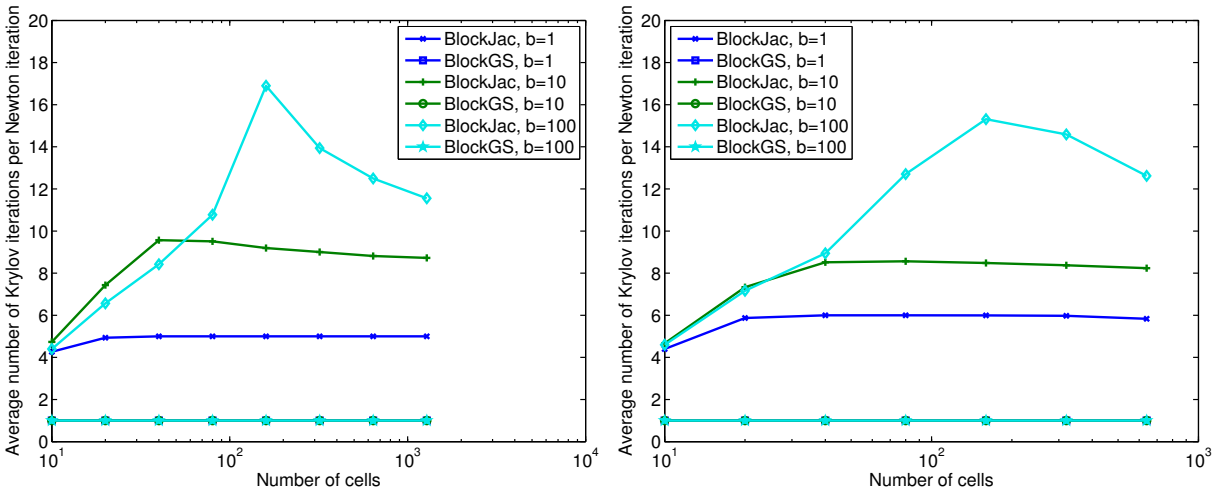

(a) $p = 1$ (b) $p = 2$

FIGURE 3. Number of Krylov iterations for (4.1) using a Roe type of diffusion with varying fast wave speed b and with different preconditioners.

As a final result in this section, we compare the computational cost of the Roe type and Rusanov type numerical diffusion operators, i.e. the average number of block Jacobi preconditioned GMRES iterations per Newton iterate vis a vis the number of cells in figure 4. The results show that in contrast to the rather low (around 10) iterations for the Roe type numerical diffusion, the number of iterations registers a very sharp increase with respect to the wave speed ratio $\frac{b}{a}$ for the Rusanov type diffusion operator. Furthermore, the piecewise quadratic version of the method with the Rusanov type diffusion operator may not even converge. Thus, this is a good example to illustrate that the Roe method, based on a characteristic decomposition of the

system, is vastly superior to an approximate characteristic decomposition such as the Rusanov type numerical diffusion operator.

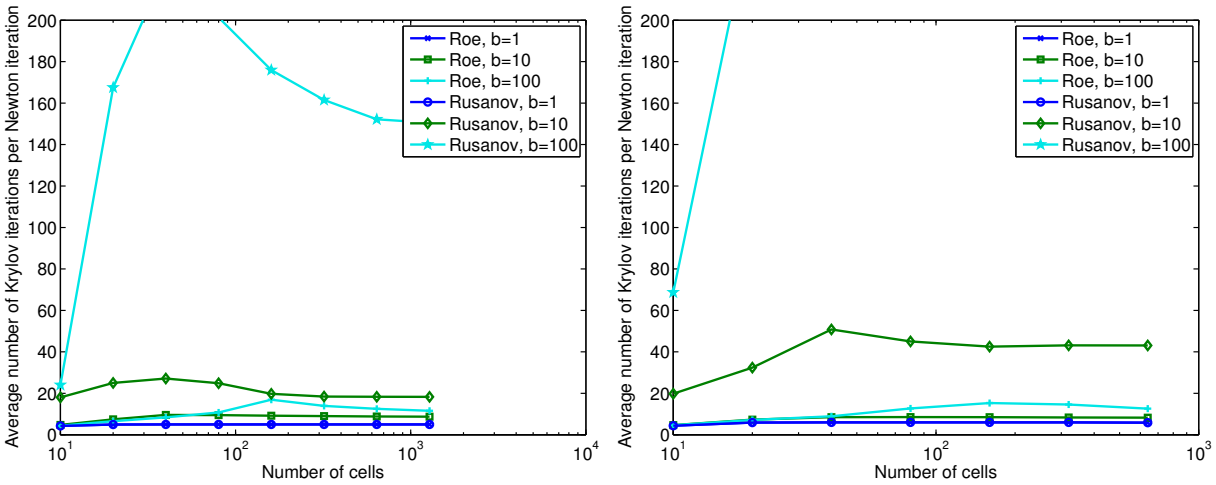

(a) $p = 1$ (b) $p = 2$

FIGURE 4. Number of Krylov iterations for the linear system (4.1) using the block Jacobi preconditioner with varying fast wave speed b and diffusive fluxes.

5. EULER EQUATIONS

For the final set of numerical experiments, we consider the compressible Euler equations of gas dynamics. In two space dimensions, the Euler equations are of the form,

$$\begin{aligned} \mathbf{U}_t + \mathbf{F}^1(\mathbf{U})_x + \mathbf{F}^2(\mathbf{U})_y &= 0, \\ \mathbf{U} &= (\rho, \rho u, \rho v, \rho E), \\ \mathbf{F}^1(\mathbf{U}) &= \left(\rho u, \rho u^2 + p, \rho uv, \rho uH\right), \\ \mathbf{F}^2(\mathbf{U}) &= \left(\rho v, \rho uv, \rho v^2 + p, \rho vH\right). \end{aligned} \tag{5.1}$$

Here, ρ is the density, u and v are the x and y components of the velocity, respectively, and ρE is the total energy. Furthermore, auxillary quantities are the pressure p, sound speed c, and the enthalpy H given by

$$p = (\gamma - 1)(\rho E - \frac{1}{2}\rho(u^2 + v^2)), \quad c = \sqrt{\gamma \frac{p}{\rho}}, \quad H = \frac{c^2}{\gamma - 1} + \frac{1}{2}(u^2 + v^2)$$

and γ is the adiabatic exponent, which is set to 1.4 (diatomic gas) in all experiments.

The Euler equations are equipped with the standard thermodynamic specific entropy $s = \log p - \gamma \log \rho$. The resulting entropy function is given by,

$$S = \frac{-\rho s}{\gamma - 1}.$$

The corresponding entropy flux functions and entropy variables can be readily calculated and are described in [13]. We will approximate the Euler equations with the streamline diffusion shock-capturing DG method (2.4). The entropy conservative flux that we use is the one designed in [25] and the numerical diffusion operators of the Roe and Rusanov type are described in [13].

5.1. **One-dimensional pulse propagation.** As a first numerical example, we consider the problem proposed by Klein in [29] as a model problem for computing the incompressible limit of the Euler equations. As in [29], we consider the one-dimensional version of the Euler equations (5.1) by setting $v = 0$ and considering only the x direction. The aim is to simulate a high amplitude, short wave length layering of the density that is set in motion by a periodic train of right-running (fast) acoustic waves.

$M = 1/51$ represents the nondimensionalisationing parameter (reference Mach number) and we consider a rescaled version of the initial data of [29] (problem II):

$$\begin{aligned} \rho(x,0) &= \bar{\rho}_0 + \Phi(x)\tilde{\rho}_0 \sin(40\pi x/L) + M\tilde{\rho}_0 \frac{1}{2}(1+\cos(\pi x/L)), \\ p(x,0) &= \left(\bar{p}_0 + M\tilde{p}_0 \frac{1}{2}(1+\cos(\pi x/L))\right)/M^2, \\ u(x,0) &= \tilde{u}_0 \frac{1}{2}(1+\cos(\pi x/L)), \end{aligned} \tag{5.2}$$

where x is in the domain $[-L, L]$ with $L = 1/M$ and

$$\bar{\rho}_0 = 1, \quad \tilde{\rho}_0 = 1/2, \quad \bar{p}_0 = 1, \quad \tilde{p}_0 = 2\gamma, \quad \tilde{u}_0 = 2\sqrt{\gamma}. \tag{5.3}$$

The function

$$\Phi(x) = \begin{cases} \frac{1}{2}(1-\cos(5\pi x/L)), & 0 \le x \le 2L/5, \\ 0, & \text{otherwise} \end{cases} \tag{5.4}$$

is used to smoothly restrict the large amplitude, short wave length density variation to the region $[0, 2L/5]$. The initial density is visualized in figure 5 (a). Periodic boundary conditions are used and the equations are solved from $t = 0$ up to $T = 5.071$. In this time span, the long wave length acoustic pulse crosses the domain about two and a half times.

As we are interested in computing the slowly moving density fluctuations, we use a discrete version of

$$\lambda_{\max}^{\text{slow}} = \max_{x\in[-L,L]} |u(x, t^n)| \tag{5.5}$$

at every time step t^n to set the time step (CFL number) as in (3.5). The resulting effective CFL number computed with (3.6) and the computed solution averages to approximately 18.

The approximate density, computed with the piecewise quadratic shock-capturing DG method (2.4) with a Roe type numerical diffusion operator and an effective CFL number of approximately 18, is shown in figure 5 (b). The exact solution is a (slow) rightward propagation of the initial short wave length density fluctuations. The computed solutions (particularly at moderate to fine resolutions) are a very good approximation of the exact solution even if the time step, being based on the slow wave speed, is quite large and does not resolve the fast moving acoustic waves. Thus, the method is quite effective at computing the density pulse.

Given the large time steps, the key contributor to the computational cost is the cost per time step. Again, the dominant factor in the cost per time step is the number of GMRES iterations per Newton step. We present the average number of GMRES iterations per Newton step in figure 6. We observe that,

- Both the block Jacobi and block Gauss Seidel preconditioners, developed in the recent paper [23], are robust in the sense that the number of iterations is constant (or even decreasing) with respect to increasing mesh resolutions or increasing polynomial degree.
- Even if the time step is quite large (effective CFL number of 18), the number of GMRES iterations with the block Jacobi preconditioner and a Roe type diffusion operator is about 20.
- The number of iterations is minuscule, about 2, for the symmetric version of the block Gauss Seidel preconditioner and the Roe type diffusion operator, making this combination a very effective computational framework.
- The Rusanov diffusion operator does not function as well. Either the number of iterations are quite high (about 120 for piecewise linear elements) or the iteration does not converge (for the piecewise quadratic elements).

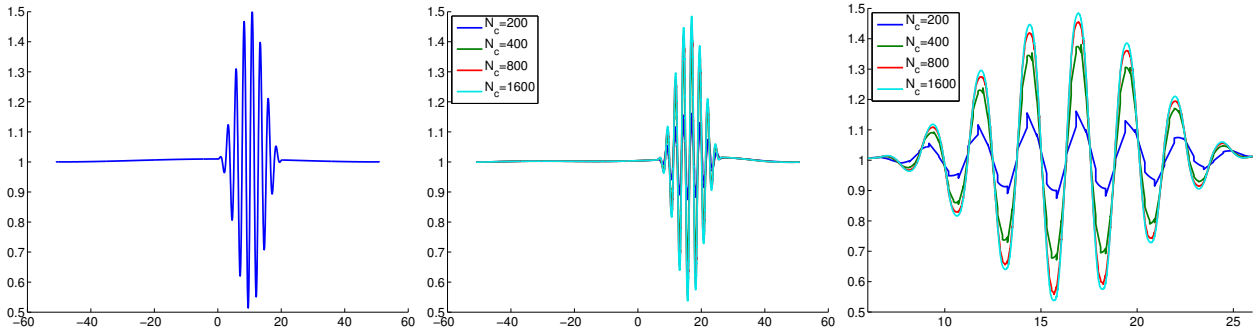

(a) $t = 0$ (b) $t = 5.071$ (c) $t = 5.071$, closeup

FIGURE 5. Approximate density for the one-dimensional pulse propagation in the Euler equations, computed initially and $T = 5.071$, with the shock-capturing DG method with piecewise quadratic elements and a Roe type numerical diffusion operator at an effective CFL number of 18.

Summarizing, we observe that the shock-capturing space-time DG method (2.4), together with a Roe type diffusion operator and a Block Gauss-Seidel (or Block Jacobi) preconditioner, is very effective at computing the slow moving density fluctuations, even for a large time step that does not resolve the time scales corresponding to the fast moving acoustic waves.

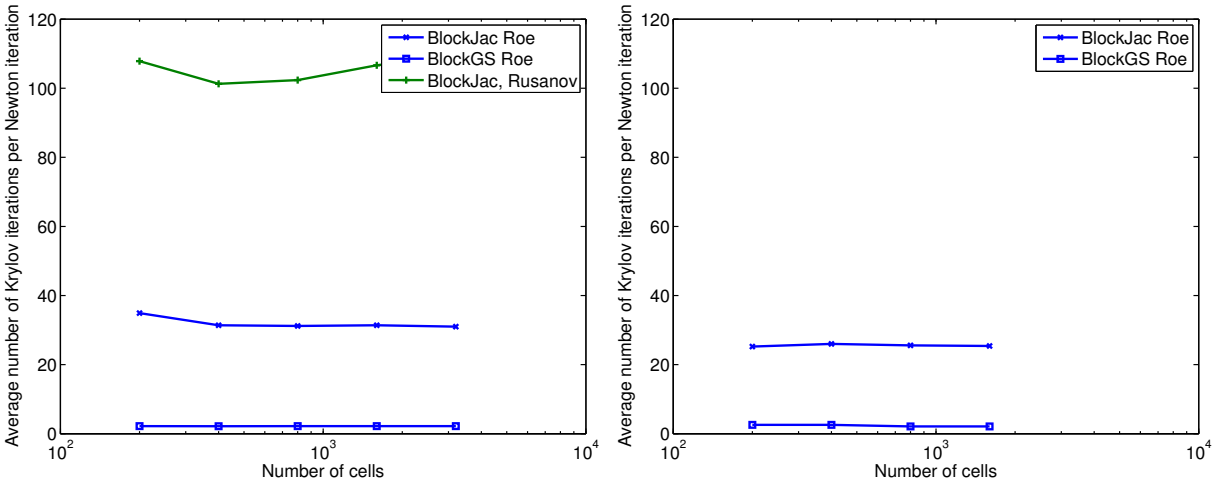

(a) $p = 1$ (b) $p = 2$

FIGURE 6. Average number of GMRES iterations for the pulse propagation problem for one-dimensional Euler equations, comparing different diffusive fluxes and preconditioners.

5.2. **Flow past a cylinder: computing the incompressible limit.** Similar to [11], we consider an Euler flow (solution of the Euler equations (5.1)) past a two-dimensional cylinder with a low free stream Mach number Ma_∞. The cylinder is centered at the origin and has diameter 1. The computational domain is bounded by an (artificial) circle of radius 10 around the origin. The following free stream variables are imposed at the outer boundary:

$$p_\infty = 101325, \quad \rho_\infty = \frac{p_\infty}{287.05 \cdot 288.15}, \quad u_\infty = \mathrm{Ma}_\infty c_\infty, \quad v_\infty = 0, \tag{5.6}$$

with $c_\infty = \sqrt{\gamma p_\infty/\rho_\infty}$.

Slip boundary conditions are imposed on the boundary of the cylinder. It is essential (particularly for computations with second and higher order polynomials) that the boundary of the cylinder is resolved accurately. To this end, we use a polynomial mapping of degree p (for $p \geq 1$) to generate curved boundary elements. The equations are solved from $t = 0$ up to $T = 0.02/\mathrm{Ma}_\infty$.

We use a Roe type diffusive flux. As we will be interested in computed the incompressible limit, we determine the time step using the slow wave speed (5.5). Then, the time step is determined using (3.5). In particular, the acoustic waves (sound speed c_∞) is ignored while determining the time step.

We will compute for three different free stream mach numbers, $\mathrm{Ma}_\infty = 0.1$, $\mathrm{Ma}_\infty = 0.01$, and $\mathrm{Ma}_\infty = 0.001$. Thus, three different regimes of moderate Mach number, low Mach number, and very low Mach number are covered in this calculation. As is well known, $\mathrm{Ma}_\infty \to 0$ is (formally) the incompressible limit of the Euler equations. Thus, we will also compute a potential flow (solution of the Laplace equation) around the cylinder to represent the incompressible limit.

We have used a reduced CFL number of $C^{\mathrm{CFL}}_{red} = 10$ to determine the time step from (3.5). From (3.6) and the computation, we report that the effective CFL numbers are 65, 590, and 6000 for the free stream Mach numbers of 0.1, 0.01, and 0.001, respectively.

The results with piecewise quadratic elements are presented in figure 7. In this figure, we have depicted the pressure coefficient,

$$c_p = \frac{p - p_\infty}{\frac{1}{2}\rho_\infty \left\|\mathbf{u}_\infty\right\|^2}$$

for the three different free stream Mach numbers. The results from figure 7 clearly show that the flow is accurately resolved, even for the lowest Mach number of 0.001 and the incompressible limit is approximated very well when the Mach number $\to 0$. Thus, the method clearly resolves the incompressible limit without any adhoc fixes.

Given the very large time steps that are associated with a very high effective CFL number of 6000, the total number of time steps is rather moderate. The computational cost per time step is determined by the number of preconditioned GMRES iterations per Newton step. The average number of multi block Gauss-Seidel preconditioned GMRES iterations are 18, 94, and 598 for Mach numbers of 0.1, 0.01, and 0.001, respectively. Thus, we see that the number of iterations increases by at most an order of magnitude even if the Mach number (and consequently the time step size (effective CFL number)) decreases (increases) by two orders of magnitude. Thus, the computational cost is still very moderate for very low Mach number flows.

In the above experiment, we have demonstrated the ability of the shock-capturing space-time DG scheme to compute low to very low mach number flows very efficiently. The scheme is of course well suited to compute moderate to high Mach number flows. As an example, we consider a flow past a cylinder with a moderate free stream Mach number of 0.75. The results (c_p), obtained with a piecewise quadratic version of the space-time DG method (2.4) and 13282 elements are shown in figure 8. The results show that the resulting transsonic flow is very well resolved with accurate and (essentially) non-oscillatory approximations of shocks. The effective CFL number in this computation is 1.6 and at most 4 block Gauss-Seidel preconditioned GMRES iterations are needed per time step. Thus, the results show that the space-time DG method is very effective and robust in computing flows with underlying Mach numbers that differ by several orders of magnitude.

5.3. **Flows past aerofoils: computing convergence to steady state.** As mentioned in the introduction, the aim of most aerodynamic computations is to accurately compute the steady state flow (cruise conditions). Although one can compute the steady state directly by solving the steady (time-independent) version of the Euler equations, it is fairly common to compute the steady state by starting with an initial condition and driving the system to steady state [26]. The transient flow need not be accurately resolved in such a computation. Given this context, convergence to steady state constitutes another set of problems where large time steps are necessary in order to accelerate convergence to steady state. The shock-capturing space-time DG method is well suited for this purpose.

In order to demonstrate the ability of the space-time DG method (2.4) to accelerate convergence to steady state, we consider an Euler flow around a NACA 0012 aerofoil [1]. The aerofoil is placed along the x axis,

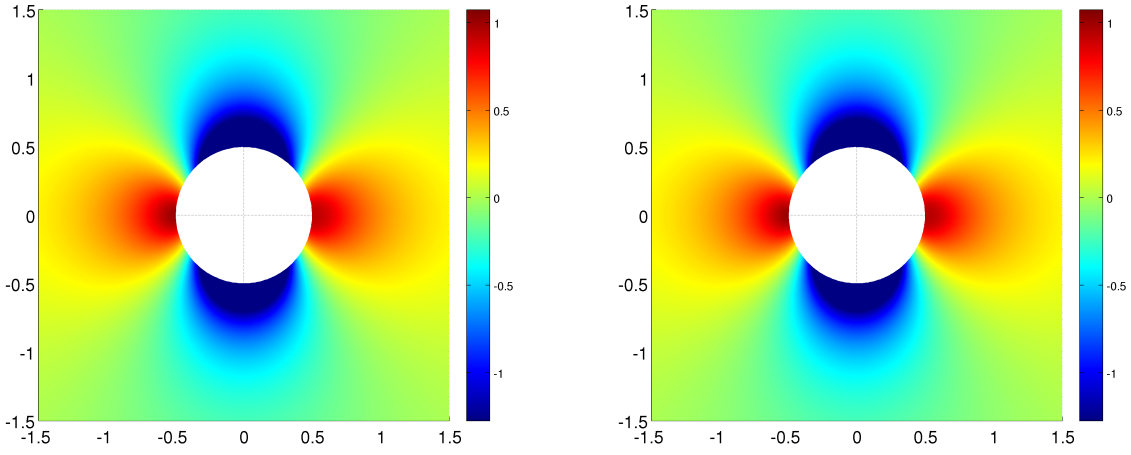

(a) $\mathrm{Ma}_\infty = 0.1$

(b) $\mathrm{Ma}_\infty = 0.01$

(c) $\mathrm{Ma}_\infty = 0.001$

(d) Incompressible limit

FIGURE 7. Pressure coefficient c_p of a flow around a cylinder at different Mach numbers, using polynomial degree $p = 2$ and $N_c = 13282$ spatial elements.

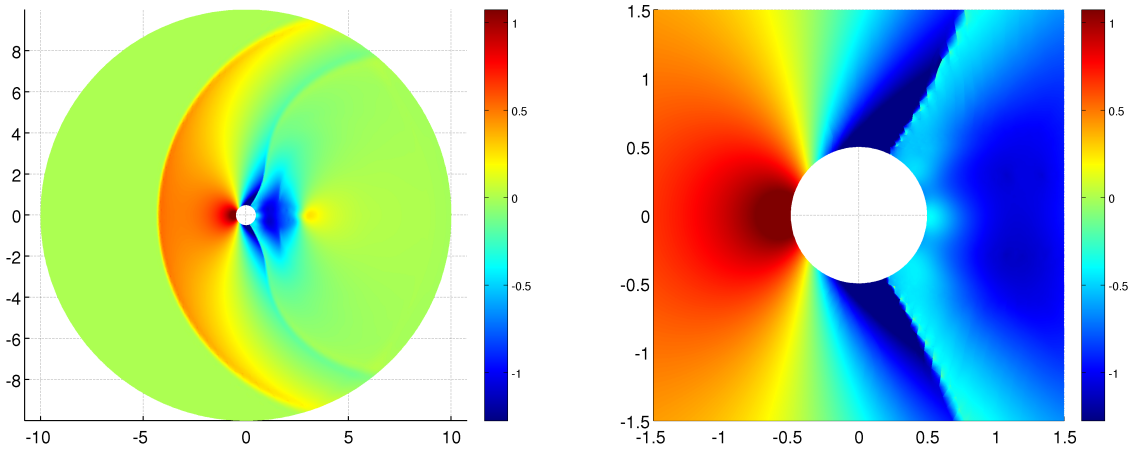

(a) Complete domain

(b) Closeup around the cylinder

FIGURE 8. Pressure coefficient of a flow around a cylinder with $\mathrm{Ma}_\infty = 0.75$ using polynomial degree $p = 2$ and $N_c = 13282$ spatial elements.

ranging from $x = 0$ (head) to $x = 1$ (tail). Slip boundary conditions are used on the aerofoil. An artificial outer boundary is placed on a circle around $(2, 0)$ with radius 4, where the following freestream values are prescribed: Mach number $\mathrm{Ma}_\infty = 0.75$, pressure $p_\infty = 8.5419$, density $\rho_\infty = 11.4452$, and an angle of attack of $4°$. We will compute and display the pressure coefficient $c_p = (p - p_\infty)/((1/2)\rho_\infty \|\mathbf{u}_\infty\|^2)$, where $\mathbf{u}_\infty$ is the freestream flow velocity. At $t = 0$, the flow is initialized by freestream values. The equations are then solved up to $t = 3.5$; the time by which the steady state is approximately reached.

An unstructured mesh (consisting of triangles) is generated around the aerofoil. This mesh is finer near the head of the aerofoil than near the tail. As a further modification, we replace the shock-capturing operator with a pressure scaled variant suggested in [22], i.e., (2.12b) is replaced by

$$D^{SC}_{n,K} = \frac{D^p_{n,K}\Delta t^n C^{SC}\overline{\mathrm{Res}}_{n,K}}{\sqrt{\int_{I^n}\int_K \left(\left\langle \mathbf{V}_t^{\Delta x}, \mathbf{U}_{\mathbf{V}}(\tilde{\mathbf{V}}_{n,K})\mathbf{V}_t^{\Delta x}\right\rangle + \sum_{k=1}^{d}\frac{\Delta x^2}{(\Delta t^n)^2}\left\langle \mathbf{V}_{x_k}^{\Delta x}, \mathbf{U}_{\mathbf{V}}(\tilde{\mathbf{V}}_{n,K})\mathbf{V}_{x_k}^{\Delta x}\right\rangle\right) dxdt + \epsilon}} \tag{5.7}$$

with

$$D^p_{n,K} = \Delta x_K^2 \frac{\frac{1}{\Delta t^n}\frac{1}{|K|}\int_{I^n}\int_K \sqrt{\sum_{k=1}^d p_{x_k x_k}^2}\, dxdt}{\frac{1}{\Delta t^n}\frac{1}{|K|}\int_{I^n}\int_K p\, dxdt}. \tag{5.8}$$

We will determine the time step using the condition (3.2) and consider four different time steps corresponding to effective CFL numbers of 0.5, 5, 50, and 500 respectively. The resulting pressure coefficient c_p, computed with piecewise linear elements is shown in figure 9. The results clearly show that increasing the time step (even by three orders of magnitude) did not result in a significant deterioration of the accuracy with which the steady state is resolved. In fact, the results obtained with a very large time step, corresponding to an effective CFL number of 500 are quite accurate and resolve the transsonic shocks as well as the smooth features of the solution rather well. Furthermore, the average number of Krylov iterations increases only moderately given the three orders of magnitude increase of the CFL number: it is 3, 6, 17, and 53 for CFL numbers of 0.5, 5, 50, and 500, respectively.

As a final numerical experiment, we show four different flows with underlying free stream Mach numbers of 0.5, 0.75, 1.3, and 3.0 and a very large time step, corresponding to an effective CFL number of 500 in figure 10.

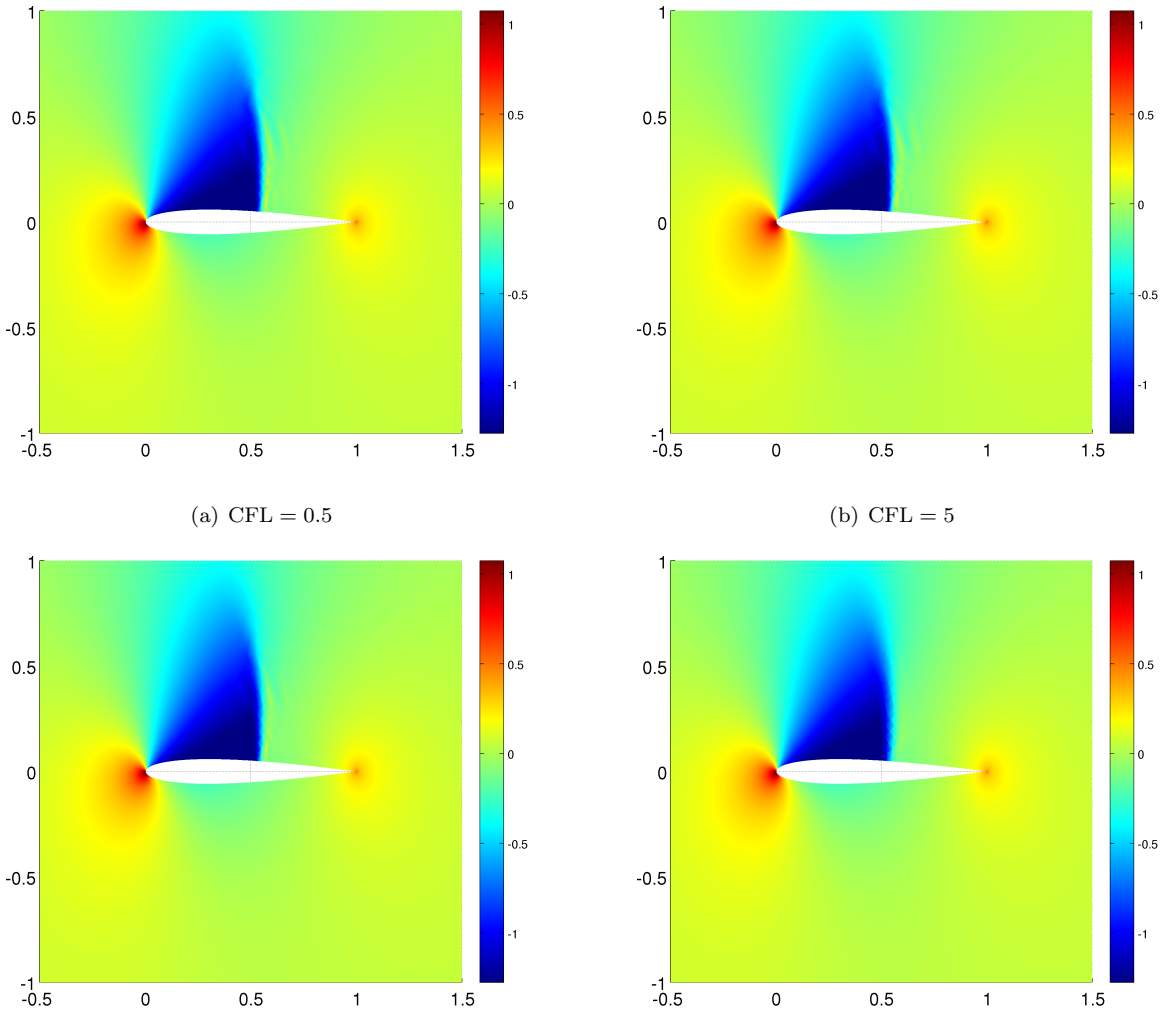

(a) CFL = 0.5

(b) CFL = 5

(c) CFL = 50

(d) CFL = 500

FIGURE 9. Pressure coefficient c_p of a $\mathrm{Ma}_\infty = 0.75$ Euler flow over a NACA 0012 aerofoil using $p = 1$ and $N_c = 16704$ at $t = 3.5$.

The results show that even for a large time step, the method resolves various regimes of flow i.e., subsonic, transsonic, and supersonic flow, very accurately, at least at the steady state. Thus, the space time DG method is well suited to approximate problems requiring rapid convergence to and high resolution of the steady state.

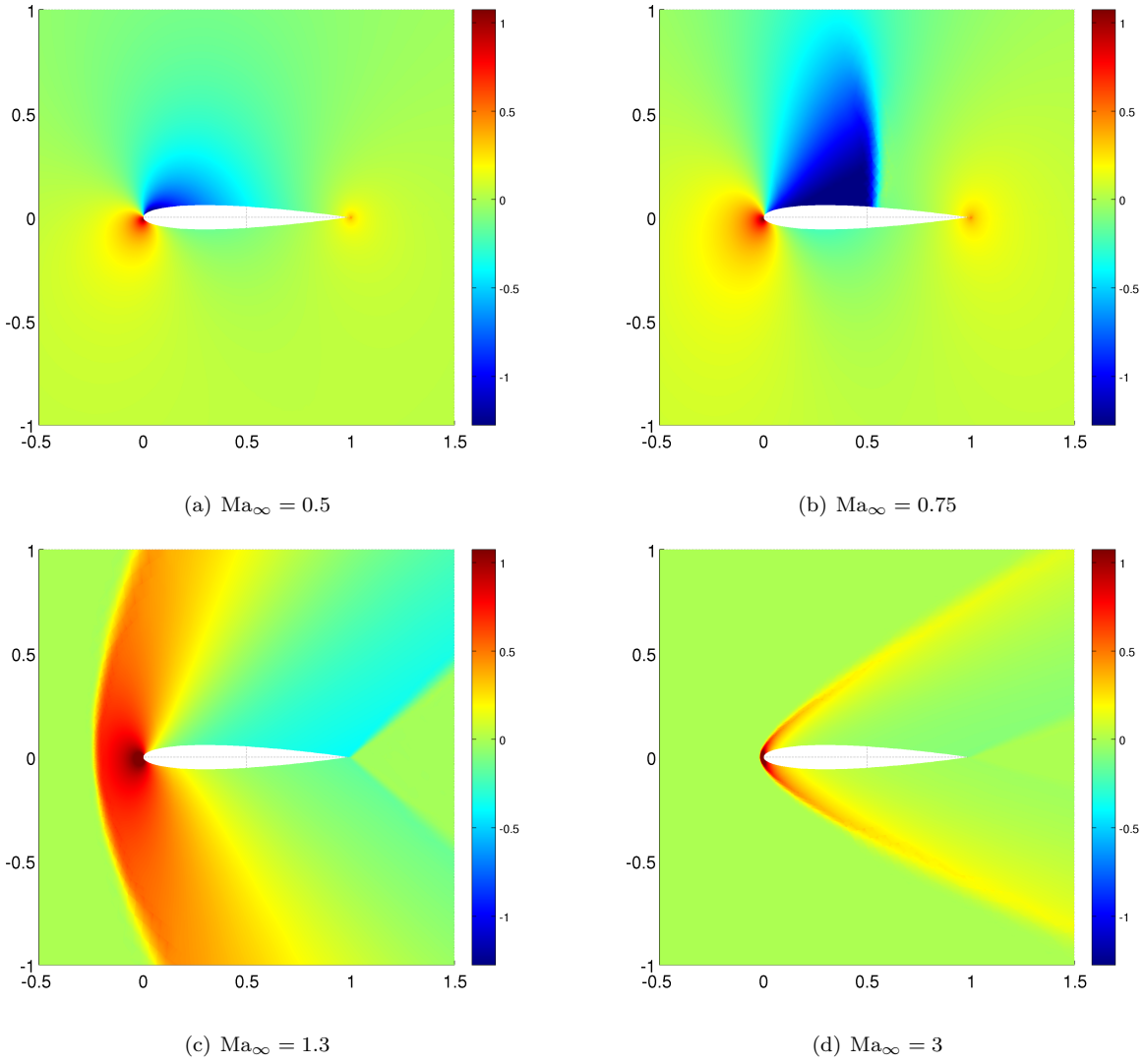

(a) $\mathrm{Ma}_\infty = 0.5$

(b) $\mathrm{Ma}_\infty = 0.75$

(c) $\mathrm{Ma}_\infty = 1.3$

(d) $\mathrm{Ma}_\infty = 3$

FIGURE 10. Pressure coefficient c_p of Euler flows over a NACA 0012 aerofoil using $p = 1$ and $N_c = 16704$ at $t = 3.5$.

6. Conclusion

Many problems of interest, modeled by systems of conservation laws (1.1), include phenomena that occur at multiple time scales. Often, the main interest in a simulation of such problems is to resolve the slow waves accurately, without requiring an accurate approximation of fast waves. Examples include the incompressible (zero Mach number) limit of the compressible Euler equations (5.1) where the interest is in resolving the matter waves, rather than the fast acoustic waves. Radiation hydrodynamics and MHD also fall into this class of problems as it is not necessary to accurately resolve the radiative waves (traveling at the speed of light) which are several orders of magnitude faster than the sonic and magneto sonic waves of interest. Furthermore, those

problems where the steady state of the flow is the object of interest also fall into this category when time stepping methods are used to drive the system into steady state. The corresponding transient need not be accurately approximated.

Standard explicit time stepping methods fail at the efficient approximation of such all speed flows as the time step is bound by the fastest time scale, leading to a prohibitively expensive method. Although many implicit and semi-implicit methods are proposed to deal with this problem, they are either tailored to a particular problem of interest or require adhoc arguments.

We present an alternative framework to compute all speed flows in this paper. Our approach is based on an entropy stable shock-capturing streamline diffusion space-time Discontinuous Galerkin (DG) method proposed in a recent paper [22]. As the space-time DG method (2.4) is unconditionally stable, one can choose suitable time steps. In particular, we choose the time step to resolve the time scales of interest by (3.4), (3.5). Consequently, the method automatically resolves the slow waves at the expense of smearing fast waves. The method is very general and requires no adhoc fixes or alterations in the code. The only change is in the CFL parameter that determines the time step.

We illustrate the method on four different sets of problems,

- A toy linear symmetric system (4.1) with two time scales.
- A one-dimensional (slow) propagation of density fluctuations in the Euler equations proposed by Klein in [29].
- A two-dimensional Euler flow past a cylinder with the specific objective of computing the incompressible (zero Mach number) limit.
- A two-dimensional Euler flow past a NACA aerofoil with the aim to computing the steady state accurately.

Based on the numerical results presented here, we conclude that the shock-capturing space-time DG method (2.4), particularly with a Roe type numerical diffusion operator and a block Gauss-Seidel type preconditioned GMRES solver, is able to

- compute the (interesting time scales) of the flow very accurately,
- is robust to several orders of magnitude variation in the Mach number, in particular it can compute the incompressible limit,
- allows for very large time steps (with effective CFL numbers running from 500 to 6000), thus resulting in significant decrease in the overall computational cost.

Hence, at one stroke, we present a method that can approximate all speed flows as well as accelerate convergence to steady state, all with reasonable computational cost. We believe that the shock-capturing DG method is particularly suitable for problems that contain multiple time scales in the system. The current paper was focussed on the two-dimensional Euler equations of hydrodynamics. Extensions to three dimensional flows, radiation hydrodynamics and magnetohydrodynamics as well as combustion will be the object of future work.

References

[1] I. H. Abbott, A. E. von Doenhoff, and L. S. Stivers. Summary of airfoil data. Technical Report 824, NACA, 1945.

[2] T. J. Barth. Numerical methods for gas-dynamics systems on unstructured meshes. In *An Introduction to Recent Developments in Theory and Numerics of Conservation Laws* pp 195–285. Lecture Notes in Computational Science and Engineering volume 5, Springer, Berlin. Eds: D. Kroner, M. Ohlberger, and Rohde, C., 1999

[3] H. Bijl and P. Wesseling. A unified method for computing incompressible and compressible flows in boundary-fitted coordinates. *J. Comput. Phys.,* 141, 1998, 153-173.

[4] B. Cockburn and C-W. Shu. TVB Runge-Kutta local projection discontinuous Galerkin finite element method for conservation laws. II. General framework. *Math. Comput.*, 52, 1989, 411–435.

[5] C. Dafermos. *Hyperbolic conservation laws in continuum physics.* Springer, Berlin, 2000.

[6] P. Degond, F. Deluzet, A. Sangam and M. H. Vignal. An asymptotic preserving scheme for the Euler equations in a strong magnetic field. *J. Comput. Phys.,* 228, 2009, 3540-3558.

[7] P. Degond and M. Tang. All speed scheme for the low mach number limit of Isentropic Euler equations. *Comm. Comput. Phys.,* 10 (1), 2011, 1-31.

[8] P. Degond, S. Jin and J. G. Liu, Mach number uniform asymptotic preserving gauge schemes for compressible flows. *Bulletin of Institute of Mathematics, Academia Sinica* New series, 2 (4), 2007, 851-892.

[9] R. J. DiPerna. Measure valued solutions to conservation laws. *Arch. Rational Mech. Anal.,* 88(3), 223-270, 1985.

[10] S. Evje and T. Flatten. CFL-violating numerical schemes for a two-fluid model. *J. Sci. Comput.,* 29 (1), 2006, 83-114.
[11] M. Feistauer, V. Dolejší, and V. Kučera. On the discontinuous galerkin method for the simulation of compressible flow with wide range of mach numbers. *Computing and Visualization in Science*, 10(1):17–27, 2007.
[12] U. S. Fjordholm, S. Mishra and E. Tadmor. Energy preserving and energy stable schemes for the shallow water equations. *"Foundations of Computational Mathematics"*, Proc. FoCM held in Hong Kong 2008 (F. Cucker, A. Pinkus and M. Todd, eds), London Math. Soc. Lecture Notes Ser. 363, pp. 93-139, 2009.
[13] U. S. Fjordholm, S. Mishra and E. Tadmor. Arbitrary order accurate essentially non-oscillatory entropy stable schemes for systems of conservation laws. *SIAM J. Num. Anal.,* 50 (2), 544-573, 2012.
[14] U. S. Fjordholm, R. Käppeli, S. Mishra and E. Tadmor. Construction of approximate solutions for hyperbolic systems of conservation laws. *Preprint,* 2014 available as arXiv:1402.0909 [math.NA].
[15] F. Fuchs, A. D. McMurry, S. Mishra and N. H. Risebro, Explicit and Implicit finite volume schemes for radiation MHD and the effects of radiation on wave propagation in stratified atmospheres, *Proc. of Hyperbolic. conference 2012*, to appear. Available as ETH SAM-reports, 2013-40.
[16] S. Gottlieb, C. W. Shu and E. Tadmor. Strong stability preserving high-order time discretization methods. *SIAM review*, 43 (1), 2001, 89-112.
[17] J. Haack, S. Jin and J. G. Liu, All speed asymptotic method for isentropic Euler and Navier-Stokes equations. *Comm. Comput. Phys.* , 12 (4), 2012, 955-980.
[18] F. H. Harlow and A. Amsden. A numerical fluid dynamics calculation for all flow speeds. J. Comput. Phys., 8, 1971, 197-213.
[19] F. H. Harlow and J. E. Welch. Numerical calculation of time-dependent viscous incompressible flow of fluid with a free surface. Phys. Fluids., 8 (12), 1965, 2182-2189.
[20] A. Harten, B. Engquist, S. Osher and S. R. Chakravarty. Uniformly high order accurate essentially non-oscillatory schemes, III. *J. Comput. Phys.*, 1987, 231-303.
[21] C. Hirsch. Numerical computation of internal and external flows. *Butterworth-Heinemann*, second edition, 2007.
[22] A. Hiltebrand and S. Mishra. Entropy stable shock-capturing space-time discontinuous Galerkin schemes for systems of conservation laws. *Numerische Mathematik*, 126(1), 103–151, 2014.
[23] A. Hiltebrand and S. Mishra. Efficient preconditioners for a shock-capturing space-time discontinuous Galerkin schemes for systems of conservation laws. *Preprint*, 2014, available as ETH SAM report, 2014-04.
[24] A. Hiltebrand. Entropy-stable discontinuous Galerkin finite element methods with streamline diffusion and shock-capturing for hyperbolic systems of conservation laws. PhD thesis, *in preparation*, 2014.
[25] F. Ismail and P. L. Roe. Affordable, entropy-consistent Euler flux functions II: Entropy production at shocks. *Journal of Computational Physics* 228(15), volume 228, 54105436, 2009.
[26] A. Jameson. Time dependent calculations using Multigrid, with applications to unsteady flows past airfoils and wings. *AIAA paper*, 1991, 91-1596.
[27] J. Jaffre, C. Johnson and A. Szepessy. Convergencea of the discontinuous Galerkin finite element method for hyperbolic conservation laws. *Math. Model. Meth. Appl. Sci.,* 5(3), 367-386, 1995.
[28] C. Johnson and A. Szepessy. On the convergence of a finite element method for a nonlinear hyperbolic conservation law. *Math. Comput.*, 49 (180), 1987, 427-444.
[29] R. Klein. Semi-implicit Extension of a Godunov-type Scheme Based on Low Mach Number Asymptotics I: One-dimensional Flow. *J. Comput. Phys.*, 121(2):213–237, Oct. 1995.
[30] R. Klein, N. Botta, T. Schneider, C. D. Munz, S. Roller, A. Meister, L. Hoffman and T. Sonar. Asymptotic adaptive methods for multi-scale problems in fluid mechanics. *J. Eng. Math.,* 83, 2001, 261-343.
[31] R. J. LeVeque. Finite volume methods for hyperbolic problems. *Cambridge University Press,* Cambridge, 2002.
[32] C. D. Munz, M. Dumbser and S. Roller. Linearized acoustic perturbation equations for low Mach number flow with variable density and temperature. *J. Comput. Phys.,* 224, 2007, 352-364.
[33] C. D. Munz, S. Roller, R. Klein and K. J. Geratz. The extension of incompressible flow solvers to the weakly compressible regime. *Comp. Fluid.,* 32, 2002, 173-196.
[34] C. W. Shu and S. Osher. Efficient implementation of essentially non-oscillatory schemes - II, *J. Comput. Phys.*, 83, 1989, 32-78.
[35] E. Tadmor. The numerical viscosity of entropy stable schemes for systems of conservation laws, I. *Math. Comp.,* 49, 91-103, 1987.
[36] E. Tadmor. Entropy stability theory for difference approximations of nonlinear conservation laws and related time-dependent problems. *Act. Numerica,* 451-512, 2003
[37] V. Titarev and E. Toro. ADER schemes for three-dimensional non-linear hyperbolic systems. *J. Comput. Phys.,* 204 (2), 2005, 715-736.
[38] D. R. van der Huel, C. Vuik and P. Wesseling. A conservative pressure-correction method for all speed flows. *Comp. Fluid.,* 32, 2003, 1113-1132.

(Andreas Hiltebrand)
Seminar for Applied Mathematics (SAM)
Department of Mathematics, ETH Zürich,
HG J 49, Rämistrasse 101, Zürich -8092, Switzerland
E-mail address: andreas.hiltebrand@sam.math.ethz.ch

(Siddhartha Mishra)
Seminar for Applied Mathematics (SAM)
Department of Mathematics, ETH Zürich,
HG G 57.2, Rämistrasse 101, Zürich -8092, Switzerland (and)
Center of Mathematics for Applications (CMA),
University of Oslo,
P.O.Box -1053, Blindern, Oslo-0316, Norway
E-mail address: smishra@sam.math.ethz.ch

Recent Research Reports

Nr.	Authors/Title
2014-07	P. Grohs and S. Keiper and G. Kutyniok and M. Schaefer Cartoon Approximation with α -Curvelets
2014-08	P. Grohs and M. Sprecher and T. Yu Scattered Manifold-Valued Data Approximation
2014-09	P. Grohs and U. Wiesmann and Z. Kereta A Shearlet-Based Fast Thresholded Landweber Algorithm for Deconvolution
2014-10	P. Grohs and S. Vigogna Intrinsic Localization of Anisotropic Frames II: α-Molecules
2014-11	S. Etter and P. Grohs and A. Obermeier FFRT - A Fast Finite Ridgelet Transform for Radiative Transport
2014-12	A. Paganini Approximate Shape Gradients for Interface Problems
2014-13	E. Fonn and P. Grohs and R. Hiptmair Polar Spectral Scheme for the Spatially Homogeneous Boltzmann Equation
2014-14	J. Dick and F.Y. Kuo and Q.T. Le Gia and Ch. Schwab Multi-level higher order QMC Galerkin discretization for affine parametric operator equations
2014-15	Ch. Schwab Exponential convergence of simplicial hp-FEM for H ¹-functions with isotropic singularities
2014-16	P. Grohs and S. Keiper and G. Kutyniok and M. Schaefer α-Molecules